ELSEVIER

PII: S0032-3861(96)01027-0

Polymer Vol. 38 No. 17, pp. 4295–4304, 1997

0032-3861/97/$17.00+0.00

N.m.r. characterization of polyethylene with emphasis on internal consistency of peak intensities and estimation of uncertainties in derived branch distribution numbers

Eddy W. Hansen*, Richard Blom and Otto M. Bade
SINTEF Applied Chemistry Oslo, PO Box 124 Blindern, N-0314 Oslo, Norway
(Received 22 May 1996; revised 12 September 1996)

A comprehensive n.m.r. characterization of a low-density polyethylene (LDPE) sample with respect to the distribution of short branches, saturated and unsaturated long branch/chain ends is presented. High precision carbon chemical shift values of all assigned resonance peaks with standard deviations of less than 0.005 ppm (at 403 K and 75 MHz carbon resonance frequency) were obtained by mathematical deconvolution of the carbon spectrum, thus enabling a differentiation not only of short branches ($C_{n<6}$) but also hexyl-, oxtyl- and longer branches). Nuclear Overhauser Enhancement (NOE) measurements revealed that less than 50% of the non-equivalent carbon nuclei experienced full NOE of 2.98 while more than 25% of the corresponding carbon nuclei showed a NOE of less than 2.75. Based on spin-lattice relaxation time (T_1) and NOE measurements a statistical evaluation showed that internal quantitative consistency between peak intensities existed only under no-NOE conditions. Derived branch distribution numbers from a set of 100 synthetic carbon n.m.r. spectra of the sample, revealed that each branch could be characterized by a Gaussian or normal distribution function. Average values and standard deviations of the branch numbers are presented. © 1997 Elsevier Science Ltd.

(Keywords: polyethylene; peak assignment; chemical shift)

INTRODUCTION

During the previous two decades quantitative analysis of branching in polyethylene (PE) has been a subject of considerable interest due to the commercial importance of these materials. A limited but relevant list of publications are cited in the list of references[1–4]. The first critical study of quantitative experimental conditions was—to our knowledge—performed by Axelson *et al.*[5] who showed that a delay time of 30 s between pulses was necessitated to prevent variable saturation of the resonances. However, these measurements were performed at 118°C and it is well known that the spin-lattice relaxation times of polymers are generally sensitive to both temperature and magnetic field strength[15]. For instance, De Pooter *et al.*[14] emphasized that a delay time of 50 s between pulses would be necessary to obtain quantitative intensity data of branched PE at 130°C.

Another issue of concern is the possibility that non-equivalent carbons in PE possess different NOE, which might seriously affect the quantitative analysis of branch distributions. This problem can be circumvented by the use of gated decoupling or chemical modification of the sample (addition of paramagnetic reagent)[16]. However, both of these techniques lower experimental efficiency in terms of the time required to obtain a spectrum since the NOE is eliminated. Different authors have claimed that all carbon nuclei in branched polyethylenes have the same NOE[7,9] suggesting that this parameter will not affect the quantitative interpretation. However, Axelson *et al.*[6] noticed that when all observed resonances were analysed, an internal inconsistency among the possible combinations of peak intensities—which should yield identical results—was found. These findings were rationalized according to an overlap of peaks originating from additional non-assigned peaks in the spectrum. Another explanation might be, however, that the NOE of the different carbon nuclei are not identical, as reported by Horii *et al.* when investigating radiation induced cross-linking of linear PE[17].

One major limitation in previous studies have been the lack of presenting uncertainties both in relaxation time measurements, NOE measurements and intensity measurements. In this work we thus concentrate on the evaluation of the internal consistency regarding peak intensities (areas) by considering both spin-lattice relaxation times and NOE factors. To optimize the determination of chemical shift and peak area measurements, the frequency spectrum will be deconvoluted, i.e. fitted to a sum of Lorenzian functions.

Also, branching distribution numbers—derived from observed n.m.r. peak intensities (areas)—will be presented, with a corresponding detailed discussion concerning the uncertainty in the derived distribution numbers. To our knowledge, the uncertainty in calculated branch distribution numbers has not been critically evaluated.

* To whom correspondence should be addressed

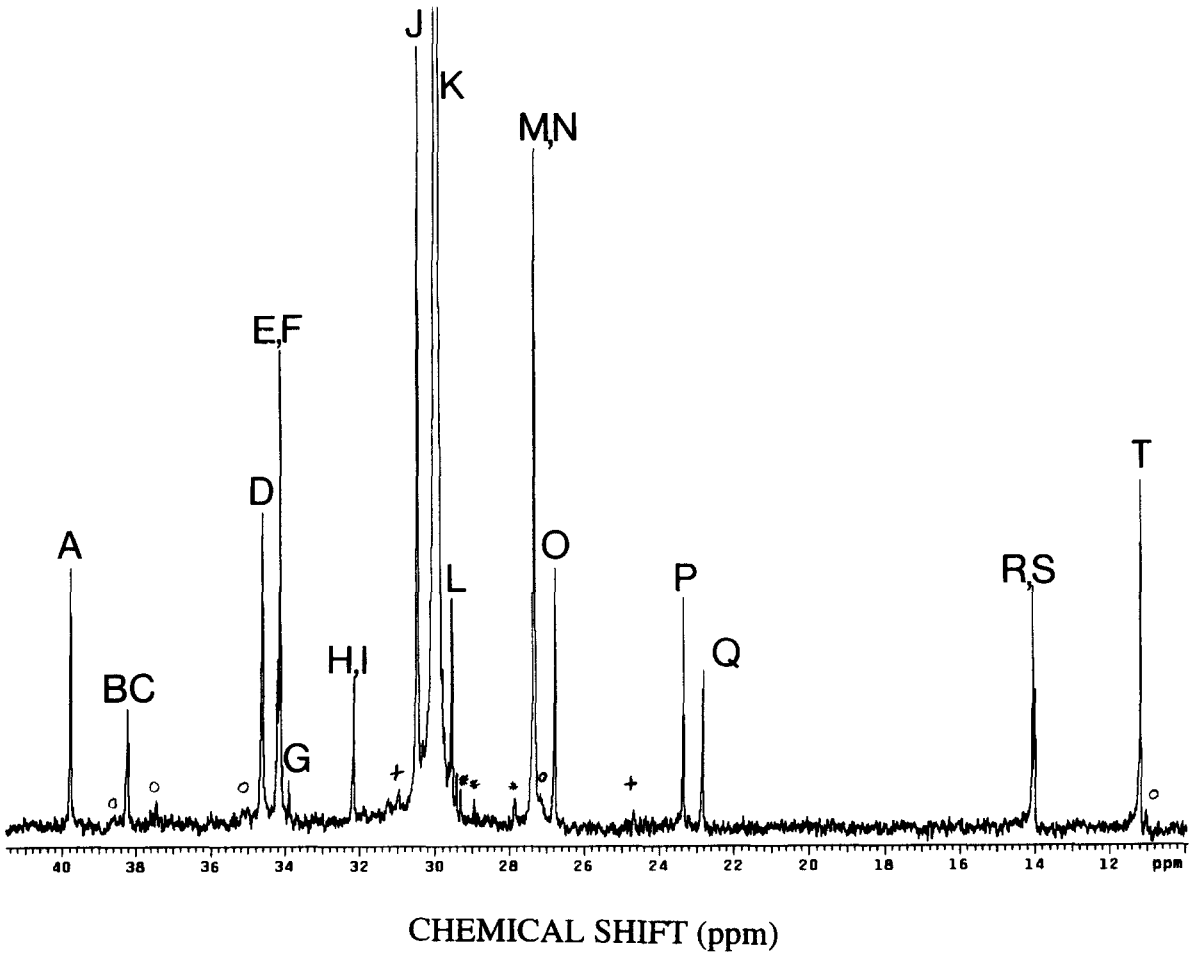

Figure 1 ^{13}C-{^{1}H} n.m.r. spectrum of a 15 wt% PE sample dissolved in ODCB. Spectrum run at 130°C. Main peak set at $\delta = 29.980$ ppm. Peaks marked with a circle (O) correspond to a composite branching of 1,3-diethyl. Peaks marked with an asterisk are not assigned. Peaks marked with (+) represent tentative assignment. See text for further details

EXPERIMENTAL

The polyethylene (PE) sample investigated in the present study was produced with a tert-butyl lithium modified Cr(II)/SiO_2 catalyst in a slurry reactor as described in ref. 18. This catalyst produces high molecular weight polyethylene with a broad molecular weight distribution as well as low molecular weight 1-olefins. The 1-olefins produced *in situ* are partly copolymerized into the polyethylene chain as to make short chain branches (SCB). G.c. analyses of the solvent phase after the polymerization shows that only linear even number 1-olefins are produced with molecular weights ranging from C_4 up to at least C_{14}.

The PE sample was dissolved in *o*-dichlorobenzene (ODCB) in a 5 mm outer diameter n.m.r. tube (approximately 15 wt% of polymer in solution) and saturated with nitrogen gas before being sealed. The polymer was dissolved at 150°C for 30 min before being run at 130°C on a Varian VXR 300 NMR spectrometer operating at 75 MHz carbon resonance frequency. A $\pi/2$-pulse was applied with an acquisition time of 2 s. The pulse repetition time was fixed at 30 s and the sweep width set to 4 kHz using 16 K data points. The free induction decay (f.i.d.) was stored in a double precision mode and Fourier transformed after being zero-filled to 256 K data points, resulting in a digital resolution of 0.031 Hz/point. If not otherwise stated, the carbon signals were sampled under ^{1}H decoupling using the WALTZ decoupling pulse sequence to remove any coupling between proton and carbon nuclei. A total of 480 transients were sampled, corresponding to a total experimental time of 4 h. Fourier transformation was performed on the final signal, after applying an exponential multiplication of the f.i.d., corresponding to a frequency broadening of 0.25 Hz. The final spectra were baseline corrected using a second-order polynomial. The area (intensity) of each peak was determined by a mathematical deconvolution, i.e. fitting the resonance peak to a Lorenzian function by a non linear least squares procedure, thus enabling an optimum value of peak position (chemical shift), linewidth and intensity (area). This procedure represents a significant improvement compared to a simple numerical integration of the resonance band, in particular when severe overlap of peaks are considered.

T_1 measurements were performed using a conventional inversion recovery pulse sequence with the proton decoupling being on only during acquisition (on NOE). The NOE factor was determined by applying a single carbon $\pi/2$-pulse with the proton decoupling turned on at a certain time (which was varied in an arrayed experiment) and remaining on until the next experiment, i.e. the proton decoupling pulse was left on also during acquisition to ensure a proton decoupled spectrum. Additional details concerning the measurement of NOE will be discussed in more detail in a later section.

Table 1 Carbon 13 peak assignment, chemical shift (δ) and linewidth ($\Delta\nu_{1/2}$) of the resonance peaks in *Figure 1* of a PE sample run at 130°C and at 75 MHz

Resonance peak	Assignment[14]	Assignment (this work)	Chemical shift (δ) (ppm)	Linewidth (Hz)
A	br. B_2		39.745 ± 0.005	2.47
B	br. B_{6+}		38.245 ± 0.010	1.92
C	br. B_4		38.204 ± 0.005	2.15
D	αB_4, αB_{6+}		34.607 ± 0.003	1.20
E	$4B_4$		34.197 ± 0.004	1.52
F	αB_2		34.118 ± 0.004	1.65
G	Vinyl (end group)		33.884 ± 0.004	2.71
H		$3B_6$	32.191 ± 0.002	0.44
I1		$3B_8$[c]	32.169 ± 0.004	0.38
I2		$3B_{longer+}$	32.156 ± 0.003	0.58
J	γB_4, γB_2, γB_{6+}		30.476 ± 0.002	1.93
K	Main chain (CH_2)		29.980 ± 0.002	2.29
L1		$3B_4$	29.550 ± 0.002	0.80
L2		$4B_6$[a]	29.536 ± 0.002	0.61
M	βB_2, βB_4, βB_{6+}		27.339 ± 0.001	1.00
N		$5B_6$[b]	27.323 ± 0.002	0.56
O	$2B_2$		26.768 ± 0.003	2.43
P	$2B_4$		23.354 ± 0.003	1.06
Q1		$2B_6$	22.859 ± 0.002	1.05
Q2		$2B_8$[c]	22.835 ± 0.003	1.01
Q2		$2B_{longer+}$	22.826 ± 0.003	1.23
R	$1B_4$		14.067 ± 0.005	1.27
S1		$1B_6$	14.024 ± 0.006	1.44
S3		$1B_{7+}$	14.003 ± 0.005	1.28
T	$1B_2$		11.173 ± 0.002	1.22

[a] Includes the γ carbon of intermediate branch lengths
[b] Includes the β carbon of intermediate branch lengths
[c] Includes the possibility of a branch near a chain end, i.e. $-CH_2CH(CH_2(CH_2)_nCH_3)CH_2CH_2CH_2CH_2CH_2CH_3$

The ^1H n.m.r. spectra were sampled using a single Bloch delay with a repetition time of 60 s between pulses to ensure quantitative sampling of the f.i.d. The acquisition time was set to 2 s with a sweep width of 5 kHz using 20 K data points.

RESULTS AND DISCUSSION

^{13}C n.m.r.-peak assignment

Figure 1 shows a proton decoupled ^{13}C n.m.r. spectrum of a 15 wt% PE dissolved in orthodichlorobenzene (ODCB) at 130°C with proton decoupling applied between successive 90° r.f.-pulses to obtain 'full' NOE. The resonance peaks or bands are denoted by capital letters from A to T with the former symbolizing the peak at the lower magnetic field. Based on chemical shift calculations (using the Lindemann and Adams rules[19]), the three low intensity peaks in the spectrum (marked with an asterisk) neither belong to a branch near the end of a chain end (carbons 1–4 from the end) nor do they belong to any composite branching,

$$-CH_2CH(CH_2(CH_2)_xCH_3)(CH_2)_nCH(CH)_2$$
$$((CH_2)_yCH_3)CH_2-$$

with $n = 1$, 3 or 5 and x, y representing integers larger than 0. These peaks therefore remain unassigned and are not encountered in this work. From the quantitative analysis performed in this work we have reason to believe that these 'unknown' structures do not have any significant impact on the results.

Of particular interest is the small resonance peak at $\delta = 11.05$ ppm which is typical of composite branching. Using the Lindemann and Adams chemical shift approximations[19] the five peaks marked with a circle (O) can be assigned to a composite branch of ethylene in a 1,3 arrangement. The assignment of these peaks are from low field to high field; C($\alpha\alpha$), C(br), C($\alpha\delta$+), C(2) and C(1). Of somewhat more speculative nature is the assignment of the resonance peaks at $\delta = 31$ ppm and $\delta = 24.65$ ppm (marked with a '+' in *Figure 1*), which might be assigned to the C($\gamma\gamma$) and C($\beta\beta$) in 1,7 and 1,5 arrangements, respectively. The latter peak might also belong to a carbonyl group situated along the main chain. However, the intensity of these ethylene branches amount to less than 5% of the total ethylene branching and are therefore not implemented in the quantitative analysis. These peaks are—in short—excluded from the present discussion.

Five replica measurements of the sample were performed and a sum of Lorenzian functions fitted to each observed spectrum by a non-linear least squares fit to obtain an optimum value of chemical shifts and line widths (at half maximum intensity). The results are summarized in *Table 1*, showing a reproducibility in chemical shift within approximately 0.004 ppm (standard

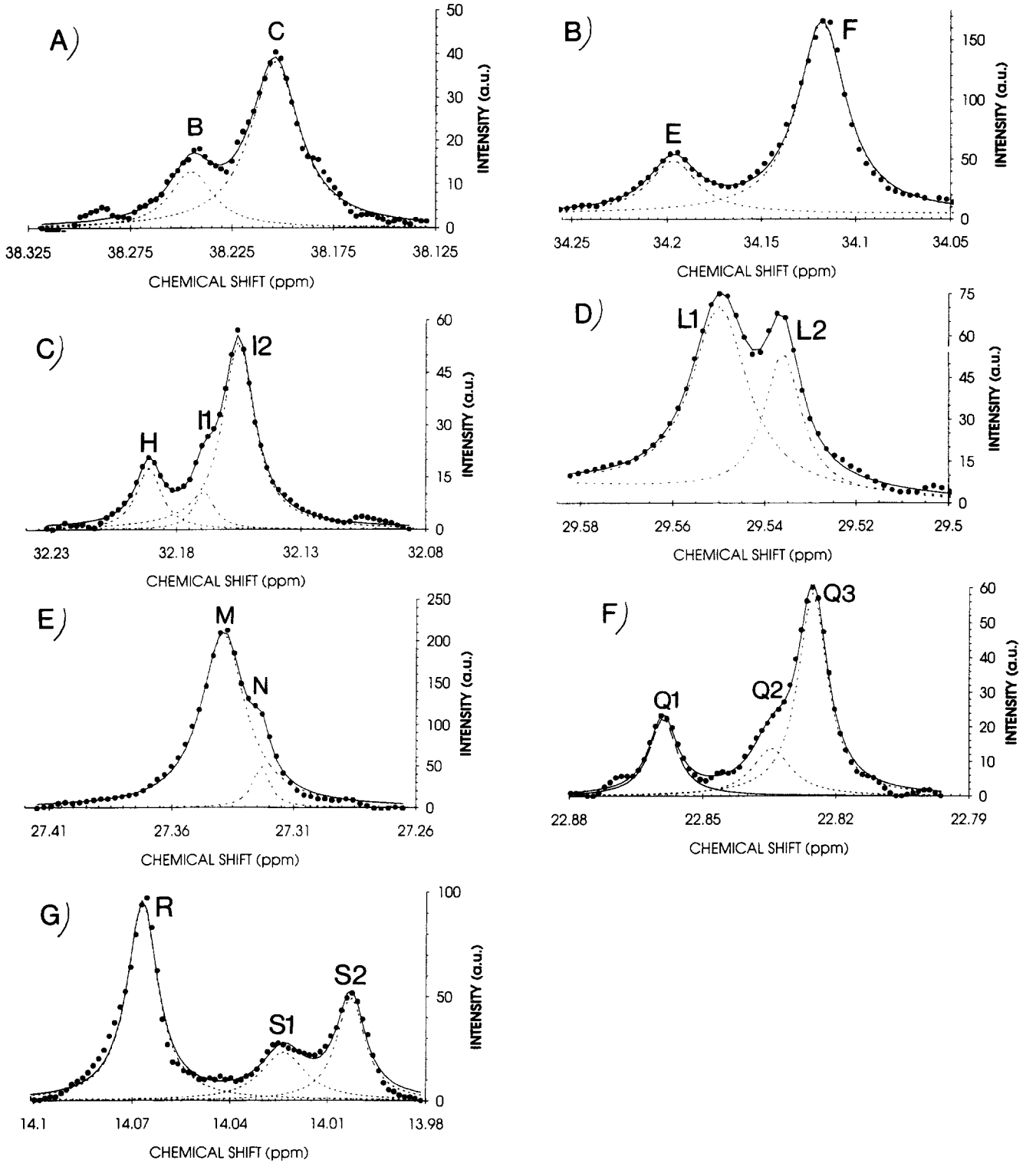

Figure 2 Expanded views of selected chemical shift regions of the spectrum shown in *Figure 1*. (A) 38.12–38.32 ppm, (B) 34.05–34.25 ppm, (C) 32.08–32.23 ppm, (D) 29.50–29.58 ppm, (E) 27.26–27.41 ppm, (F) 22.79–22.88 ppm and (G) 13.98–14.10 ppm. The dashed curves represent deconvoluted Lorenzian functions. The solid curve represents the overall fit

deviation), corresponding to 0.3 Hz in frequency units. The most recent work—to our knowledge—which suggests to present chemical shift values of the same order of precision as in this work is reported by De Pooter *et al.*[14] who investigated ethylene copolymers dissolved in the same solvent (ODCB) and at the same temperature (130°C), but at a lower magnetic field strength, corresponding to 50 MHz carbon resonance frequency. Their digital resolution of 0.5 Hz indicates an uncertainty of approximately 0.007 ppm in chemical shift estimation (if no curve-fitting is applied, which was not reported). We have used their results to assign the peaks in the spectrum of *Figure 1*. The results are summarized in *Table 1*, columns 2 and 3.

The nomenclature used in this work is that of Usami and Takayama[9] where isolated branches are described by xB_n, where n is the length of the branch and x is the carbon number starting with the methyl group as '1'. For

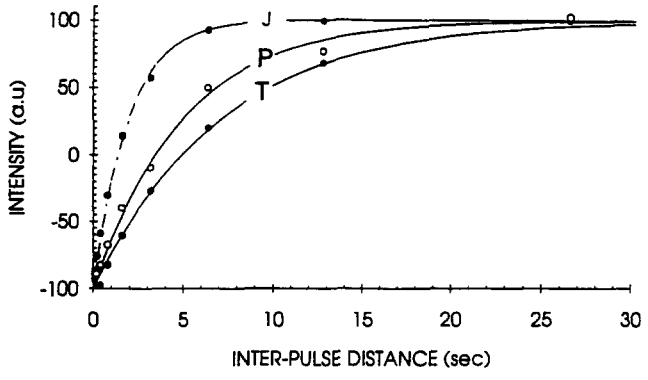

Figure 3 Longitudinal magnetization vs inter-pulse timing in an inversion recovery pulse sequence of peaks J, P and T of *Figure 1* at 130°C. Solid curves represent non-linear least squares fit of equation $I = I_0[1 - 2\exp(-\tau/T_1)]$ to the observed data, with τ representing the inter-pulse timing

Table 2 Spin-lattice relaxation times (T_1) and Nuclear Overhauser Enhancement factors (f). See text for further details

Resonance peak	T_1 (s)	f
A	2.36 ± 0.9	3.09 ± 0.09
B	1.55 ± 0.14^a	2.68 ± 0.09
C	1.55 ± 0.14^a	2.87 ± 0.02
D	1.20 ± 0.04	3.07 ± 0.18
E	1.52 ± 0.08	2.62 ± 0.16
F	1.65 ± 0.03	3.13 ± 0.12
G	3.78 ± 0.48	2.67 ± 0.45
H, I1, I2	9.52 ± 0.61^b	2.97 ± 0.10
J	1.93 ± 0.04	2.47 ± 0.07
K	2.29 ± 0.03	2.67 ± 0.02
L1, L2	4.28 ± 0.16^c	2.58 ± 0.06^g
M, N	1.82 ± 0.04^d	2.71 ± 0.01^h
O	1.99 ± 0.06	2.92 ± 0.02
P	4.95 ± 0.20	3.05 ± 0.04
Q1, Q2, Q3	8.27 ± 0.85^e	2.77 ± 0.04^i
R	8.87 ± 0.29	2.61 ± 0.06
S1, S2	15.5 ± 0.7^f	2.65 ± 0.05^j
T	7.1 ± 0.081	2.96 ± 0.09

[a–f] Peaks could not be reliably separated from the spectrum. T_1 represents an 'average' value

[g–j] Peaks could not be reliably separated from the spectrum. f represents an 'average' value

example $1B_4$ designates the methyl in a butyl branch. For the backbone carbons, the Greek letters and 'br' are used instead of x for methylenes and a branch point, respectively.

An excellent linear correlation between De Pooter's reported chemical shift data and the chemical shift values presented in this work is found. The correlation coefficient was 0.999989 with a standard deviation of 0.010 ppm, corresponding to a difference between the two sets of chemical shift data of less than 0.2%. Within a 95% confidence interval the two sets of chemical shift data are identical. However, their chemical shift values were systematically smaller 0.071 ± 0.010 ppm, which is explained by the much higher concentration of polymer used in their work (approximately 20 wt% compared to the approximately 15 wt% in this work). Also, De Pooter used a mixture of solvents (either ortho-dichlorobenzene or trichlorobenzene) which might affect the chemical shift. Moreover, De Pooter has used 30 ppm as a reference whereas 29.98 ppm has been used in this work.

The resonance peaks reveal linewidths of approximately 1.5 Hz (*Table 1*) which represents an exceptionally good spectral resolution. The spread in linewidth suggests, however, that peak heights cannot be used in quantitative analysis. For instance, resonance peak A has a linewidth which is nearly five times larger than resonance peak N. *Figure 2A* shows that resonance peaks originating from the branch carbons of butyl branches and longer branches—with a shift difference of only 3 Hz—can be easily separated at 75 MHz resonance frequency. Moreover, the resonance peaks from the α carbons in ethyl branches and the inner carbon of a butyl branch ($4B_4$) with a shift difference of less than 6 Hz are almost completely separated (*Figure 2B*). In a paper published by Bugada *et al.*[11], a small splitting of the $3B_6$ and $3B_{n>6}$ was detected when the spectrum was run without NOE. A corresponding splitting under complete proton decoupling was reported to be unobservable. *Figure 2C* shows the same chemical shift region in the spectrum presented in this work (with 'full' NOE) and signifies a clear splitting of these same two peaks. In fact, a shoulder (I1) at the low field side of resonance peak I2 can be inferred from this spectrum, suggesting the existence of intermediate chain lengths (>6) to exist. From the method described to produce the polymer, these intermediate branches are assigned to C8 branches. However, it is also possible that the peaks assigned to these intermediate branches could be a branch near the chain end, i.e. $-CH_2CH(CH_2(CH_2)_nCH_3)CH_2CH_2CH_2CH_2CH_2CH_3$. At least, we do not have any reasons for eliminating this possible structure. In the rest of this discussion we will use the term intermediate branch to mean C8 or a branch near the chain end, as just referred to. This same kind of splitting can be seen in *Figure 2F* and *Figure 2G* of resonance peaks Q_i and S_i, respectively, and shows that resonance lines separated by less than 2 Hz can be resolved. A complete assignment of resonance peaks in the spectrum of *Figure 1* are summarized in *Table 1* and will be used in the quantitative analysis which will be presented in a later section.

Spin-lattice relaxation time

A quantitative analysis of spectral lines necessitates knowledge about spin-lattice relaxation times and NOE factors. The former were measured using a conventional inversion recovery pulse sequence with proton decoupling being on only during acquisition, i.e. under no NOE conditions. An example is shown in *Figure 3* for resonance peaks J, P and T which represent short, intermediate and long relaxation times. A complete list of relaxation times are presented in *Table 2*. Although it was possible to separate overlapping peaks—as discussed in the previous section—it was difficult to obtain reliable T_1 data for these same peaks. Instead, the total spectral intensity of these specific chemical shift regions was used in determining an 'average' T_1 of the respective peaks. However, noting that these overlapping spectral regions represent peaks from carbons which are nearly equivalent with respect to geometrical environment, the T_1 times are presumably not significantly different. We have therefore tentatively assumed that they are identical. Many groups have reported spin-lattice relaxation times in PE[5,7,14] and have shown T_1 to be strongly dependent on both temperature and on applied magnetic field strength[15]. Again, De Pooter *et al.*[14] have published relaxation times of copolymers at

Table 3 Observed (I_{obs}) and calculated (I_{calc}) peak intensities under Nuclear Overhauser Enhancement (NOE) conditions

Resonance peak	I_{obs}	95% Confidence interval of I_{obs}	I_{calc}[a]	TEST[b]
A	309	303–315	264	–
B	42.1	37.5–46.7	32.5	–
C	138	135–141	155	–
D	513	501–524	408	–
E	167	161–172	155	–
F	593	583–603	528	–
G	31.7	27.2–36.2	31.7	+
H, I1, I2	155	147–164	158	+
J	872	858–886	936	–
K	13245	13197–13293		
L1, L2	254	236.1–271.6		
M, N	892	877–907	936	–
O	302	294–310	264	–
P	154	147–160	155	+
Q1, Q2, Q3	155	149–161	158	+
R	170	162–177	155	+
S1, S2	164	155–174	158	+
T	266	258–274	264	+

[a] Calculated by solving equations (2a)–(2q). See text for further details
[b] Consistency test. +/– indicates that calculated results are within/outside the experimentally determined 95% confidence interval

Table 4 Observed (I_{obs}) and calculated (I_{calc}) peak intensities without Nuclear Overhauser Enhancement (NOE)

Resonance peak	I_{obs}	95% Confidence interval of I_{obs}	I_{calc}[a]	TEST[b]
A	100	92–108	93.6	+
B	15.7	8.0–24	15.0	+
C	51.9	48.2–56	57.6	(+)
		46.8–57.0[c]		
D	167	144–189	160	+
E	63.6	54.9–72.4	57.6	+
F	190	173–206	187	+
G	11.9	5.9–17.8	11.9	+
H, I1, I2	60.7	55.7–65.5	59.5	+
J	353	332–375	348	+
K	4956			
L1, L2	98.5			
M, N	335	306–352	348	+
O	101	89–113	93.6	+
P	50.4	45.2–55.5	57.6	(+)
		46.9–57.9[c]		
Q1, Q2, Q3	56	52.6–59.5	59.5	+
R	65	63.6–71.9	57.6	(+)
		57.9–72.1[c]		
S1, S2	61.8	58.4–65.2	59.5	+
T	89.8	84.6–94.9	93.6	+

[a] Calculated by solving equations (2a)–(2q). See text for further details
[b] Consistency test. +/– indicates that calculated results are within/outside the experimentally determined 95% confidence interval
[c] Uncertainties in T_1 are included

the same temperature (130°C) as in this work, but at a lower magnetic field strength, corresponding to a carbon resonance frequency of 50 MHz. The spin-lattice relaxation times presented in this work were linearly correlated with the corresponding T_1 data published by De Pooter *et al.* with a correlation coefficient of 0.9853 and a standard deviation of approximately 0.28 s. However, our measurements are systematically larger by about 16%, which could be related to the larger magnetic field applied in this study. Approximating the overall spin-lattice relaxation rate by a simplified Bloembergen–Purcell–Pound expression: $1/T_1 \approx K[\tau/(1+\omega^2\tau^2)]$ where K is a constant and τ represents the overall correlation time of the motion, this equation would predict an overall correlation time of approximately $\tau = 2.3$ ns when considering a difference in spin-lattice relaxation times at 50 MHz and 75 MHz of approximately 16%. We have seen reports of correlation times an order of magnitude less[15], suggesting that the difference in magnetic field strength cannot be the main cause of the difference observed in spin-lattice relaxation times. However, noting that the polymer concentration in our work is approximately 15 wt% and the corresponding concentration in De Pooter's work is approximately 30 wt%, we believe that this effect is the main reason for the discrepancy in spin-lattice relaxation times observed between De Pooter and our work. A higher concentration would certainly favour a smaller spin-lattice relaxation time[15]. Moreover, an exceptionally large relaxation time (15.5 ± 0.7 s) was found for the methyl group carbons of long branches which was nearly 50% larger than reported by De Pooter *et al.* This relaxation time was thus excluded from the linear correlation fit discussed above.

Nuclear Overhauser Enhancement (NOE)

It has generally been assumed that the NOE is complete and identical for all carbons in PE[5,9]. However, Axelson *et al.*[6] reported that an inconsistency existed when different combinations of peak intensities in the spectrum were compared. Due to the exceptionally high resolution in the spectrum obtained in this work, we found it advantageous to measure NOE and to investigate the internal consistency in peak intensities (area) with and without NOE.

NOE was measured by allowing the longitudinal carbon magnetization to relax towards equilibrium without proton decoupling for a time τ_1 after the initial r.f.-pulse. After this time period, the proton decoupling was turned on and remained on for a time period $\tau_2 + t_a$, where t_a defines the acquisition or sampling time. The signal was thus acquired under complete proton decoupling conditions. Using the theory outlined in ref. 20 an expression relating the peak intensity (I) to the time parameters τ_1, τ_2, t_a and the intensities I_{NOE} (equilibrium magnetization under 'full' NOE) and I_0 (equilibrium magnetization without NOE),

$$I = I_{NOE} - (I_{NOE} - I_0)\exp\left(-\frac{\tau_2}{T_1}\right) - I_0\exp\left(-\frac{\tau_1+\tau_2+t_a}{T_1}\right) \quad (1a)$$

Since $\tau_1 + \tau_2 + t_a = 30$ in this experiment, equation (1a) can be simplified to involve only τ_2 and T_1 as time parameters, i.e.

$$I = I_{NOE} - (I_{NOE} - I_0)\exp\left(-\frac{\tau_2}{T_1}\right) - I_0\exp\left(-\frac{30}{T_1}\right) \quad (1b)$$

Equation (1b) can in general be used to obtain both the spin-lattice relaxation time, T_1, as well as the intensities I_{NOE} and I_0 by measuring I vs τ_2. We have, however, used the T_1 values from *Table 2* when fitting equation (1b) to the observed data in order to increase the degrees of freedom in the fit. The results are summarized in *Table 3* (I_{NOE}) and *Table 4* (I_0), which includes the 95% confidence interval for the estimated signal intensities. *Figure 4* illustrates how the signal intensity varies with

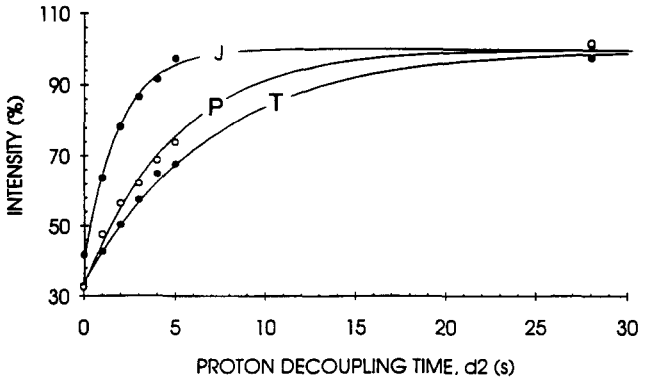

Figure 4 Signal intensity vs proton decoupling time (τ_2) of peaks J, P and T at 130°C. The solid curves represent non-linear least squares fit of equation (3) to the experimental data. See text for further details

the proton decoupling time (τ_2) for the same three peaks (J, P and T) as presented in *Figure 3* for the inversion recovery experiment.

Also, the NOE-factor (f) has been determined by replacing I_0 with I_{NOE}/f in equation (1b) resulting in

$$I = I_{NOE}\left\{\left(1-\frac{1}{f}\right)\exp\left(-\frac{\tau_2}{T_1}\right)-\frac{1}{f}\exp\left(-\frac{30}{T_1}\right)\right\} \quad (1c)$$

For each resonance line, T_1 (*Table 2*) and I_{NOE} (*Table 3*) were inserted into equation (1c) and f determined by fitting this equation to the observed (τ_2, I)-data by a non-linear least squares fit. The results are summarized in *Table 2*. The NOE factor determined for the methylene carbons in vinyl chain ends ($-\underline{C}H_2-CH=CH_2$) was too unreliable to have any significance.

The important conclusion to be made from these measurements is that—within a 95% confidence interval—approximately half of the resonance lines in *Figure 1* reveal a theoretical maximum NOE factor of 2.98, while more than 25% of the peaks exhibit a NOE factor of less than 2.75. This might have significant impact on the quantitative analysis, and in particular on the branch distribution derived from peak intensity measurements of spectra acquired under 'full' NOE conditions. This will be the subject in the next section.

Quantitative analysis of ^{13}C n.m.r. spectra consistency test

In order to check the internal consistency of observed resonance peak intensities one must keep in mind that some non-equivalent carbon nuclei in the polymer contribute—accidentally—to the same resonance peak in the spectrum. Before discussing these equations in more detail some formal definitions need to be clarified. A differentiation is made between carbon nuclei belonging to long saturated branch ends (LBE) and long saturated chain ends (LCE). Likewise, long chain branches containing unsaturated branch ends are denoted VBE, while unsaturated chain ends are denoted VCE. In contrast to long chain ends, branch ends will give rise to additional resonance peaks in the spectrum from the branch carbon and the neighbouring α, β and γ backbone carbons. For instance, resonance peak 'B' in the spectrum originates from both saturated and unsaturated long chain branch carbons resulting in the equation $I_B = k(N_{LBE} + N_{LVE})$ where I_B denotes the n.m.r. signal intensity of peak B and N_{LBE} and N_{LVE} represent the number of saturated and unsaturated long branches, respectively. The parameter k is a proportionality constant. Likewise, resonance peak 'D' originates from α carbons of butyl and long chain branches giving rise to the equation $I_D = k(2N_B + 3N_{LBE} + 3N_{LVE})$ where N_B represents the number of butyl branches. The integers (2 and 3) result from the contribution of two equivalent α carbons in the butyl branch and three equivalent α carbons from LBE and LVE, respectively. A list of relevant equations are summarized below;

$$I_A = kN_E \quad (2a)$$

$$I_B = k(N_{LBE} + N_{VBE}) \quad (2b)$$

$$I_C = kN_B \quad (2c)$$

$$I_D = k(2N_B + 3N_{LBE} + 3N_{VBE}) \quad (2d)$$

$$I_E = kN_B \quad (2e)$$

$$I_F = 2kN_E \quad (2f)$$

$$I_G = k(N_{VCE} + N_{VBE}) \quad (2g)$$

$$I_{H,I} = k(N_{LBE} + N_{LCE}) \quad (2h)$$

$$I_J = k(2N_E + 2N_B + 3N_{LBE} + 3N_{VBE}) \quad (2j)$$

$$I_{M,N} = k(2N_B + 2N_E + 3N_{LBE} + 3N_{VBE}) \quad (2k)$$

$$I_O = kN_E \quad (2l)$$

$$I_P = kN_B \quad (2m)$$

$$I_Q = k(N_{LBE} + N_{LCE}) \quad (2n)$$

$$I_R = kN_B \quad (2o)$$

$$I_S = k(N_{LBE} + N_{LCE}) \quad (2p)$$

$$I_T = 2kN_E \quad (2q)$$

These 16 equations involve six unknowns and represent thus an over-determined set of linear equations. The parameter k is of importance when determining relative branch numbers. However, when checking the internal consistency in peak intensities (areas), this parameter can be set to an arbitrary number. We have chosen $k = 1$ and solved equations (2a)–(2q) by a linear-programming technique known as the simplex method[20] that iteratively solves a set of linear equations in a finite number of steps under necessary boundary conditions—if necessary. Since the branch numbers N_i (i = B, E, LBE, LCE, VBE and VCE) must be non-negative, the boundary conditions $N_i \geq 0$ were applied. The determined N_i values were inserted into equations (2a)–(2q) to obtain 'calculated' intensity values, I_i^{calc} (i = A–T), which were compared with the corresponding observed intensities, I_i^{obs}. The results are summarized in *Table 3* (with NOE) and in *Table 4* (no NOE). As can be seen from *Table 3* (with NOE), less than half of the calculated intensities, denoted by a + sign, fall within the 95% confidence interval of the observed intensities, indicating a poor internal consistency in observed intensities. However, when correcting for NOE effects (*Table 4*) only three of the intensities (C, P and R) fall outside of the corresponding 95% confidence intervals. Keeping in mind that the confidence intervals have been determined by assuming 'error-free' T_1 measurements, the 95% confidence intervals of peaks C, P and R were recalculated, by taking into account the error in T_1 (*Table 2*). The results are shown in *Table 4*. The observed intensities are

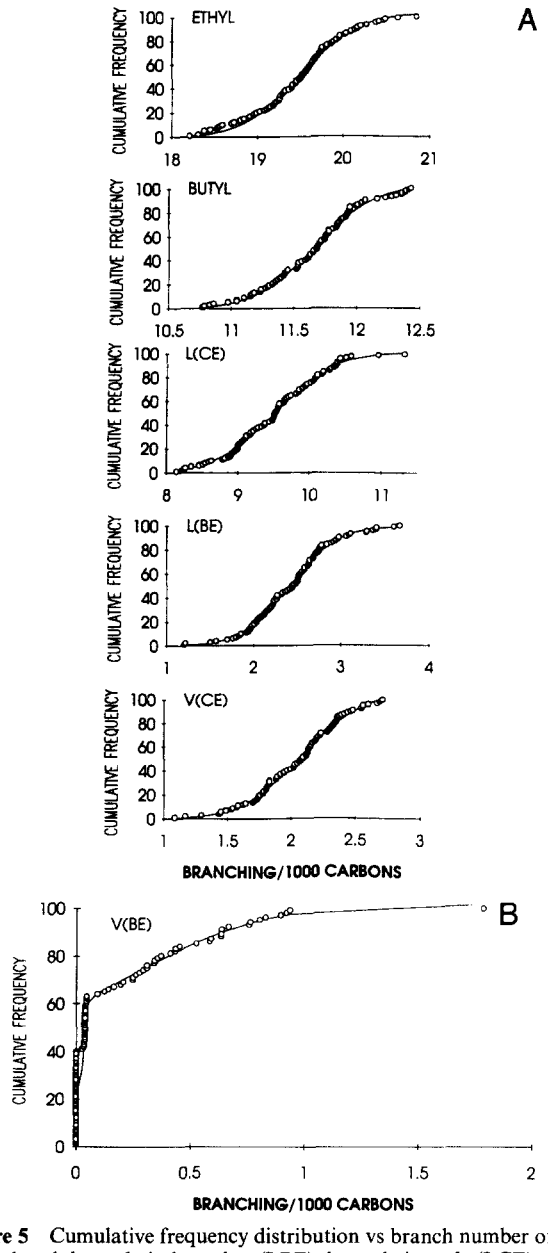

Figure 5 Cumulative frequency distribution vs branch number of (A) ethyl, butyl, long chain branches (LBE), long chain ends (LCE), vinyl chain ends (VCE) and (B) vinyl branch ends (VBE). Solid lines represent model fits to equation (3). See text for further details

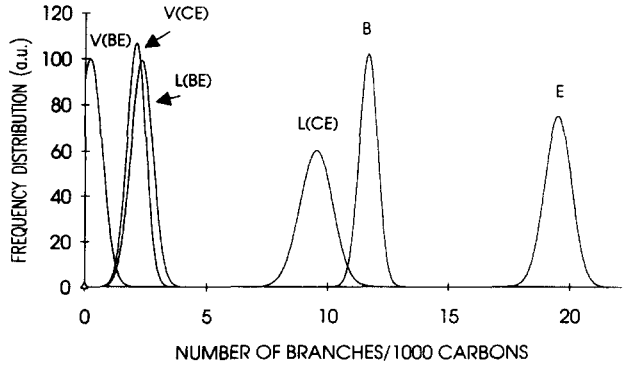

Figure 6 Frequency distribution of branches of ethyl (E), butyl (B), long chain branches (LBE), long chain ends (LCE), vinyl chain ends (VCE) and vinyl branch ends (VBE)

Table 5 Average branch number ($\bar{X}$) and corresponding standard deviation $\sigma_{\bar{X}}$ in branch number per 1000 carbon atoms, as determined from equation (3). See text for further details

Branch type	$\bar{X}$; no NOE	$\sigma_{\bar{X}}$; no NOE	$\bar{X}$; with NOE[a]
E	15.16	0.19	16.47
B	9.76	0.21	9.66
LCE	7.90	0.38	8.02
LBE	1.95	0.30	1.88
LBE + LCE (hexyl)[b]			2.0 ± 0.2
LBE + LCE (octyl)[b]			1.6 ± 0.2
LBE + LCE (long)[b]			6.4 ± 0.2
VCE	1.54	0.30	1.74
VBE	0.25	0.21	0.12

[a] Determined by the data in *Table 3* under NOE conditions
[b] Determined from peaks H, I1, I2, Q1, Q2, Q3, S1 and S2 in *Figures 2C, 2F* and *2G*

so close to the corrected 95% confidence intervals, that we conclude; the peak intensities derived from using no NOE are internally consistent.

These results suggest that differences in NOE between carbon nuclei are responsible for the internal inconsistency in intensities when 'full' NOE experiments are performed. These data do not imply that 'full' NOE experiments cannot be used to obtain quantitative results, but that the actual peaks (or carbon nuclei) to be selected should have the same NOE. For instance, a combination of peaks A, D, F, H, O, P and T could be used.

Determination of branch distribution

The number of different branches per for instance 1000 carbon nuclei, N_i' (i = B, E, LBE, LCE, VBE and VCE) can easily be derived from the formula $N_i' = 1000N_i/I_{K+}$, where I_{K+} is the signal intensity of the main peak K in addition to the signal intensities of the α, β and γ carbon resonances (with $k = 1$) and N_i is derived from equations (2a)–(2q) ($k = 1$). We are—in particular—interested in estimating the uncertainty in the derived branch numbers N_i which arises from error-propagation from the measured peak intensities I_i [i = A–T, equation (2)]. We have therefore generated 100 synthetic data sets randomly, where each set is composed of 16 intensities I_A–I_T, by assuming each intensity I_i (i = A–T) to be normally distributed with a standard deviation determined experimentally (compare the 95% confidence intervals in I_i as summarized in *Table 4*). For obvious reasons we have chosen the intensities in *Table 4*, which correspond to 'no-NOE' experimental conditions. For each of the 100 synthetic data sets the branch numbers have been calculated from equation (22) by the simplex procedure as just outlined (see previous section). The calculated cumulative frequency distributions of each branch is plotted in *Figure 5A* and fitted to equation (3),

$$F = 100 \int_0^N \frac{1}{\sigma\sqrt{2\pi}} \exp\left(-\frac{(X-\bar{X})^2}{2\sigma^2}\right) dX \qquad (3)$$

where N represents the branch number, $\bar{X}$ the average branch number and σ the standard deviation in branch number. Equation (3), which represents a normal or Gaussian frequency distribution function, fits the 'experimental' data well and suggests that each branch can be expressed by an average branch number $\bar{X}$ with standard deviation σ. The numerical results are

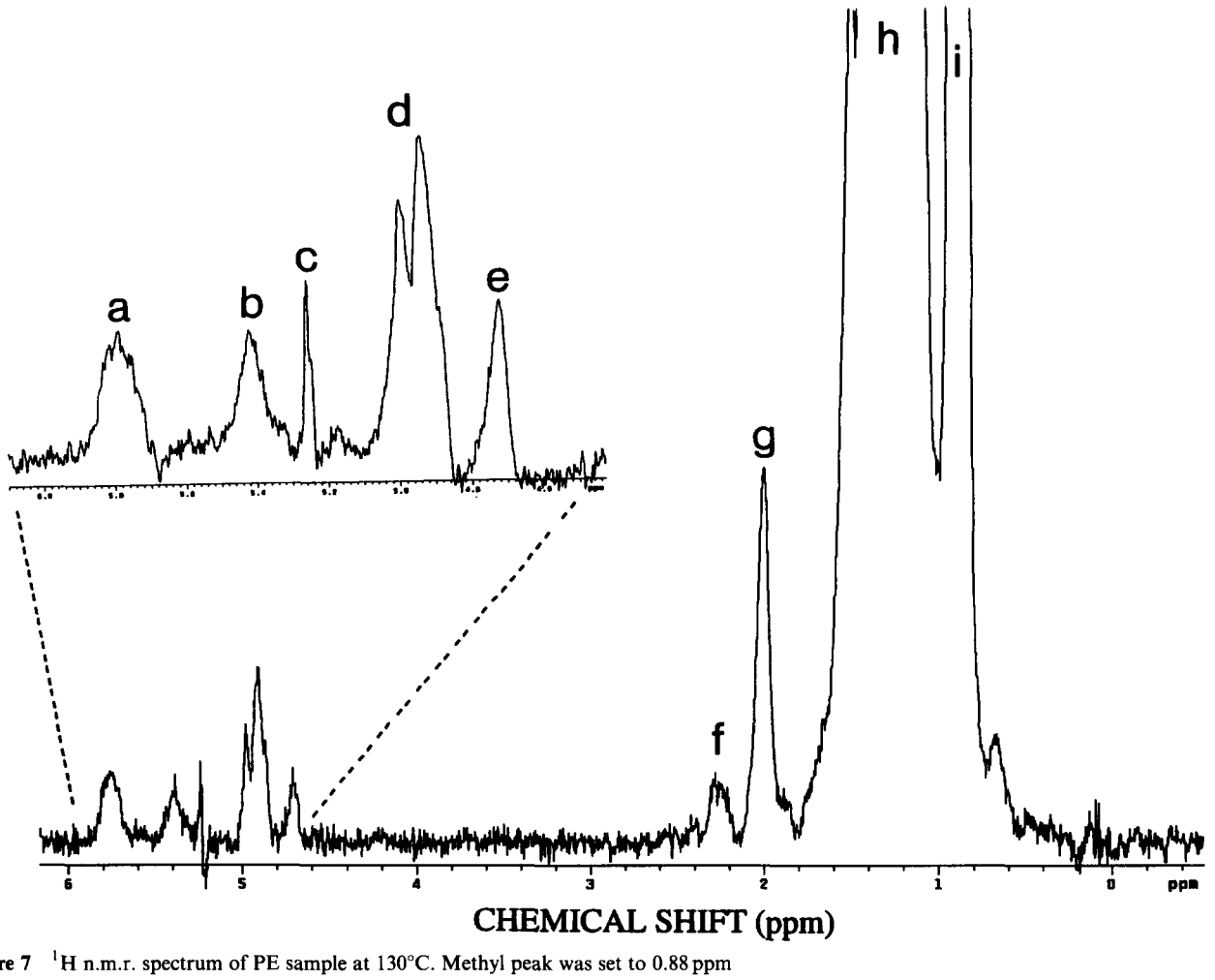

Figure 7 ^{1}H n.m.r. spectrum of PE sample at 130°C. Methyl peak was set to 0.88 ppm

Table 6 Peak assignment, chemical shift, intensity and branch distribution derived from the ^{1}H n.m.r. spectrum in *Figure 7*

Molecular fragment	Chemical shift (ppm)		Intensity y	Branch distribution per 1000 carbons
$RC\underline{H}=CH_2$	5.8	(a)	31.8	1.75
$RCH=C\underline{H}_2$	4.9	(d)	63.0	
$C\underline{H}_2=C\underline{H}_2$	5.25	(c)	6.9	0.10
$R_1R_2C=C\underline{H}_2$	4.7	(e)	12.1	0.34
$RC\underline{H}=CHR$	5.4	(b)	19.7	0.55
$RC\underline{H}_2C=C$	1.9–2.4	(f, g)	94.8	2.63
$-C\underline{H}_2-$	1.27	(h)	35115	
$-CH_2C\underline{H}_3$	0.88	(i)	2295	42.5

presented in *Table 5*. Equation (3) seems to give a poorer fit to the observed cumulative frequency distribution derived for long chain vinyl branches (VBE, *Figure 5B*) compared to the other branches and needs some additional comments. The poorer fit is caused by the fact that the synthetic data generated for this branch by applying the simplex method is restricted to positive branch numbers. Since this branch number is rather close to 0, the simplex method might actually give negative results if the restriction of positive branch numbers was omitted. However, because of this restriction, any negative number obtained during the iteration procedure would be forced to 0 and thus give rise to some 'artefacts' in the derived frequency distribution.

In conclusion, the fitted data depicted in *Figure 5* support the conclusion that the derived branch numbers are normally distributed (*Figure 6*) with average values and corresponding standard deviations presented in *Table 5*.

A surprising observation is that branch numbers derived from NOE experiments (*Table 5*, column 4) are in surprisingly good agreement with corresponding branch numbers derived from 'no-NOE' experiments, in particular when considering that a poor consistency in peak intensities was found in this former case. In fact, only the number of ethyl branches deviates significantly (10%) in the two measurements. This might be accidental, or caused by a kind of self-adjusting, self compensating mechanism when solving the over determined set of equations (2a)–(2q). This needs additional work to sort out and will not be discussed any further in this report.

The number of hexyl-, octyl- and long-branches can be estimated from the integrals of the deconvoluted spectra shown in *Figures 2C*, *2F* and *2G* by correcting these integrals for the NOE factor (f) given in *Table 2*. These integrals represent eight equations in three unknowns and can be solved by the simplex procedure as discussed in the previous section. The result of this calculation gives 2.0 ± 0.2, 1.6 ± 0.2 and 6.4 ± 0.2 for the number of hexyl-, C8- and long-branches/chain ends per 1000 carbon atoms, respectively. Likewise, the integrals of the deconvoluted carbon spectra depicted in *Figures 2D* and *2E*, support the assignment of peaks L1, L2, M and N in *Table 1*. The number average molecular weight (M_n) of the polymer is given by $M_n = 28\,000/(N_{LCE} + N_{VCE})$ which amounts to approximately 2500 ± 180.

^1H n.m.r.

The resonance peak in the ^{13}C n.m.r. spectrum at $\delta = 33.884$ ppm shows that a certain amount of vinyl chain ends (2–3 per 1000 carbon atoms) are present in the polymer. To obtain a better quantitative estimate of these 'vinyl' branches a ^1H n.m.r. spectrum of the sample was run (*Figure 7*). The expanded region in *Figure 7* shows the resonance peaks in the olefin region and was obtained by homodecoupling the intense main chain methylene proton peak at $\delta = 1.27$ ppm. The peaks, or resonance bands are identified by small letters a–i. In order to ensure quantitative sampling of the spectrum the spin-lattice relaxation time was measured. The longest T_1 time was determined for the $RC\underline{H}{=}CH_2$ protons of approximately 15 s. The intensity was measured by numerical integration of each band. Since the resolution was too poor to obtain any coupling information, the different resonance peaks (or bands) were tentatively assigned by their chemical shift values. The assignment and intensities are summarized in *Table 6*.

The corresponding number distribution of these fragments per 1000 carbon atoms was determined from the intensity data by taking into account the number of protons contributing to each peak (or band) resonance. The results are included in *Table 6* and confirms the internal consistency in peak or band intensities as seen by the relations (1) 'f + g' ≈ 'b' + 'e' + 2/3 'd + e', and (2) 'd' ≈ 2 'a'. The small letters within quotation marks represent intensities of the respective peaks or bands assigned in *Figure 7*. Moreover, the number of vinyl end groups per 1000 carbons was estimated to be 1.75, which is in agreement with 1.54 ± 0.30 as determined from ^{13}C n.m.r. In order to obtain a more reliable value of the fraction of methyl and methylene protons (F), the spectrum of the shift range 0–2.5 ppm was fitted to a sum of three Lorenzian functions resulting in a F-value of 0.052. This value corresponds to a total number of branches per 1000 carbons of 35. The uncertainty in this number is probably around 10% and is consistent with the value of 34.7 ± 0.56 as determined from ^{13}C n.m.r.

CONCLUSION

High precision chemical shift values of carbon resonance peaks of short (ethyl, butyl) and longer (hexyl, octyl, long) branches with standard deviations of less than 0.005 ppm have been obtained by mathematical deconvolution of the carbon n.m.r. spectrum. The significantly high resolution spectra enabled quantitative differentiation between hexyl branches, intermediate branches and longer branches and chain ends. Nuclear Overhauser Enhancement (NOE) measurements revealed that less than 50% of the non-equivalent carbon nuclei experienced full NOE of 2.98 while more than 25% of the carbon nuclei showed a NOE of less than 2.75. Based on spin-lattice relaxation time (T_1) and NOE measurements a statistical evaluation showed that internal quantitative consistency between peak intensities existed only under 'no-NOE' conditions. Derived branch distribution numbers from a set of 100 synthetic carbon n.m.r. spectra of the sample, revealed that each branch could be characterized by a Gaussian or normal distribution function. Average values and standard deviations of the branch numbers could be estimated. The number of vinyl branches derived from carbon n.m.r. and proton n.m.r. was identical—within experimental error. Proton n.m.r. improves the quantification of non-saturated fragments in the polymer, and of particular importance, in a much shorter experimental time.

REFERENCES

1. Randall, J. C., *J. Polym. Sci.*, 1973, **11**, 275.
2. Cudby, M. E. A. and Bunn, A., *Polymer*, 1976, **17**, 345.
3. McRae, M. A., *Makromol. Chem.*, 1976, **177**, 449.
4. Baker, C. and Maddams, W. F., *Makromol. Chem.*, 1976, **177**, 449.
5. Axelson, D. E., Mandelkern, L. and Levy, G. C., *Macromolecules*, 1977, **10**, 557.
6. Axelson, D. E., Levy, G. C. and Mandelkern, L., *Macromolecules*, 1979, **12**, 41.
7. Randall, J. C. and Hsieh, E. T., *NMR and Macromolecules*, ACS Symposium Series 247, ed. J. C. Randall. Am. Chem. Soc., Washington, DC, 1984, Chap. 9.
8. Freche, P. and Grenier-Loustalot, M.-F., *J. Eur. Polym.*, 1984, **20**, 31.
9. Usami, T. and Takayama, S., *Macromolecules*, 1984, **17**, 1756.
10. Cheng, H. N., *Polym. Bull.*, 1986, **16**, 445.
11. Bugada, D. C. and Rudin, A., *Eur. Polym. J.*, 1987, **23**, 809.
12. Usami, T., Gotoh, Y., Takayama, S., Ohtani, H. and Tsuge, S., *Macromolecules*, 1987, **20**, 1557.
13. Randall, J. C., *J. Macromol. Sci.-Rev. Macromol. Chem. Phys. (C)*,, 1989, **29**, 201.
14. De Pooter, M., Smith, P. B., Dohrer, K. K., Bennett, K. F., Meadows, M. D., Smith, C. G., Schouwenaars, H. P. and Geerards, R. A., *J. Appl. Polym. Sci.*, 1991, **42**, 399.
15. Delpuech, J.-J. (ed.), *Dynamics of Solutions and Fluid Mixtures by NMR*. John Wiley and Sons, England, 1995.
16. Bovey, F. A., *Nuclear Magnetic Resonance Spectroscopy*, 2nd edn. Academic Press, Inc., London, 1988.
17. Horii, F., Zhu, Q., Kitamoru, R. and Yamaoka, H., *Macromolecules*, 1990, **23**, 977.
18. Bade, O. M. and Blom, R., *J. Appl. Cat.*, 1997, in press..
19. Lindemann, L. P. and Adams, J. Q., *Anal. Chem.*, 1971, **43**, 1245.
20. Harris, R. K., *Nuclear Magnetic Resonance Spectroscopy, a Physical View*. Pitman Books Limited, London, 1983.
21. Hay, J. N., Mills, P. J. and Ognjanovic, R., *Polymer*, 1986, **27**, 677.